

Practical design of Ku band Vivaldi antenna array

Jakub Prouza, Zbyněk Raida¹

In the paper, a practical design of a Ku-band Vivaldi antenna array for compact radar system is presented. The realized gain, the beam width, polarization purity and the possible electronic beamforming in the horizontal plane were the most important requirements. Since the array was requested to show an enhanced mechanical stability, a novel geometry of elements was proposed. The Vivaldi slot was created on two substrates connected by metallic vias suppressing surface currents, and the microstrip feeder was placed in-between those substrates. Simulations are based on special approach in CST Microwave using infinite array of antenna elements, which should reduce computing time.

Key words: antenna array, Ku band, Vivaldi antenna

1 Introduction

The Vivaldi antenna array is requested to provide a high gain and an exactly given shape of the radiation pattern. Antenna elements for vertical and horizontal polarizations have to be separated, and the beam control in the horizontal plane has to be provided by relative phase shifting between the adjacent elements. The beam width in the horizontal plane should be around 5°. As the array will be used in compact radar system, there is also request to be as small as possible with power dividing system creating one block. This work is a part of research and development of a new radar system, so not all details and results can be published as they are part of intellectual property.

Vivaldi antennas were firstly described by Peter J. Gibson in 1979 [1]. These antennas belong to a group of slot antennas with longitudinal radiation [2]. The Vivaldi antenna is created by an exponentially tapered slot in a metallic layer (on a surface of a microwave substrate).

Both sides of the Vivaldi slot antenna can be created by a single metallic layer [3] on one side of a microwave substrate, or the antenna can be antipodal (sides of the slot are placed on different surfaces of a microwave substrate [2]). The antipodal design suffers from a higher cross-polarization.

In order to reduce the cross-polarization, the balanced antipodal Vivaldi antenna was designed [4] using an additional substrate. On the new substrate, the metallic side of the slot from the top surface is mirrored.

The low limit of the operation frequency is related to the width of the aperture. The Vivaldi antenna is linearly polarized with electric field intensity vector parallel to the slot plane.

In the open literature, several papers on the design of Ku-band Vivaldi arrays can be found.

In [5], authors discussed a linear array of antipodal elements with an overlap broadening the impedance bandwidth of the array. Due to the antipodal structure, polarization purity was not sufficient.

In [6], the exponentially tapered slot on the top side of the substrate was excited by a microstrip transmission line on the bottom side. Authors discussed practical issues of the design and fabrication of a dual-polarized array consisting of 128 elements. Attention was turned to the light weight and compact size.

In [7], an array of 4×4 Vivaldi elements was designed. On sides next to the tapered slot, grooves on both sides of the exponentially tapered slot were etched to suppress surface currents and improve both impedance and radiation characteristics of the antenna.

The practical design presented in the paper was aimed to develop a Vivaldi array with high polarization purity (the antipodal structure was denied), suppressed surface currents (metallic vias on side walls were used) and increased mechanical stability (two-substrate Vivaldi elements with a microstrip excitation in between were developed). According to our knowledge, such a concept has not been published in the open literature yet.

The design of a single antenna element is described, and several configurations of the antenna array are discussed, and the feeding network is presented before the prototype of the array is shown.

2 Vivaldi antenna array

The designed Vivaldi element is created by an exponentially tapered slot etched into a metallic film on one surface of a microwave substrate. The element is fed by a microstrip line and a terminating stub on the opposite side of the substrate (see Fig. 1).

¹ Fakulta elektrotechniky a komunikačních technologií VUT v Brně, xprouz03@vutbr.cz, raida@feec.vutbr.cz

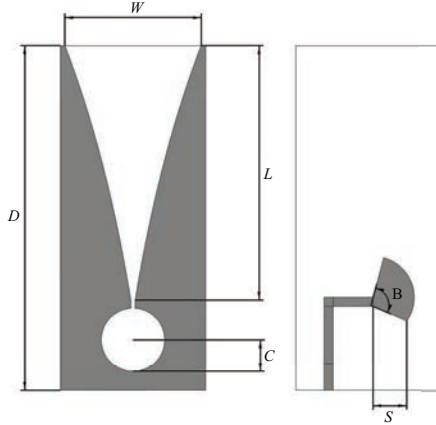


Fig. 1. Layout of Vivaldi element (left), top side with Vivaldi slot (right) bottom side with microstrip feeder

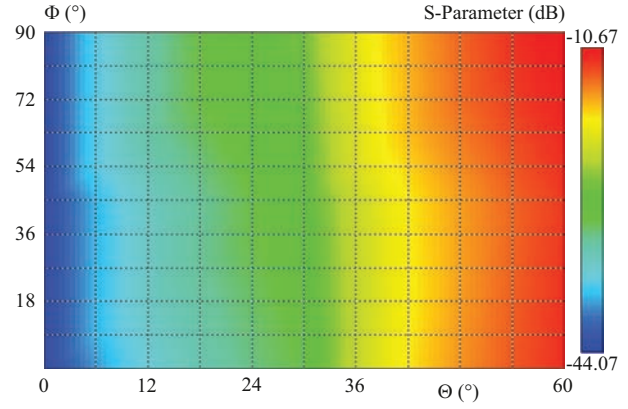


Fig. 2. Dependency of active reflection coefficient on frequency and scanning angle

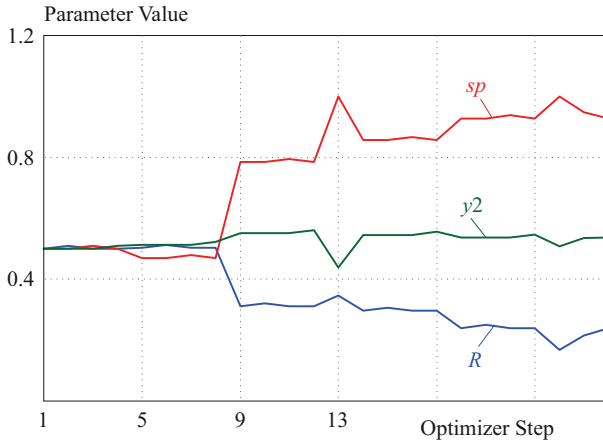


Fig. 3. Converging of optimized parameters

When designing an array, mutual coupling between elements has to be considered, including the effect of conductive connections among neighbouring antennas.

In simulations, the following formula can be used to calculate reflection coefficient of elements in the array [8]

$$\Gamma_{\text{act}} = \sum_{n=1}^N S_{mn} \frac{a_n}{a_m}. \quad (1)$$

Here, m and n are numbers of elements in an array, a_n is excitation coefficient and S_{mn} is the coupling coefficient.

Equation (1) can be extended by parameters of scanning angles in case of a phased antenna array, and the active reflection coefficient can be depicted in form of a colour map (the value of coefficient is expressed depending on frequency and scanning angle as shown in Fig. 2). Here, we can obtain reflection coefficient for the whole frequency band by the worst-case method. And the extracted reflection coefficient can be used as a parameter of the objective function in optimization.

- Opening rate R : the parameter of the exponentially tapered slot influencing matching in the whole frequency band. It affects the shape of the slot, which

is given by the following equation (2) published for example in [3]:

$$y = C_1 e^R x + C_2. \quad (2)$$

Here, C_1 and C_2 are given by (3) and (4) so the flare goes through the both end points (x_1, y_1) and (x_2, y_2) :

$$C_1 = \frac{y_2 - y_1}{e^{R x_2} - e^{R x_1}}, \quad (3)$$

$$C_2 = \frac{y_1 e^{R x_2} - y_2 e^{R x_1}}{e^{R x_2} - e^{R x_1}}. \quad (4)$$

In these equations, ending points (y_1, y_2) also define the length of the tapered slot.

- Slot aperture W : the parameter determines the lowest operation frequency and is also given by the ending points (x_1, x_2) .
- Spacing between elements SP : the parameter should be $\lambda/4$ approximately for the highest frequency. SP affects the virtual waveguide created by the grid of antenna elements.

The array of Vivaldi radiators was modelled in CST Microwave Studio and optimized by the default Trusted region method. In comparison with Particle swarm optimization and Newton method, Trusted region was able to converge to the opti-mal solution in about 15 steps. Other two optimization methods needed more steps to find optimal values. As an optimized parameter were chosen parameters above. Below is a graph exported from CST Microwave showing converging of these pa-rameters with method of trusted region, see Fig. 3.

The unit cell the entire antenna array is formed from, consists of two identical antenna elements mutually rotated for 90° . That way, both required polarizations are obtained, see Fig. 4.

For a better mechanical stability of the array, the antenna element was manufactured from two layers of a microwave substrate. On each substrate, identical exponential slots on the metalized surface were etched. The feedline was designed on the common surface of layers,

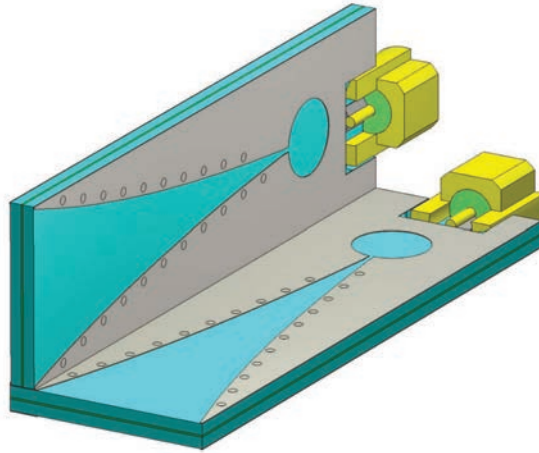


Fig. 4. Cell of antenna array providing dual polarization

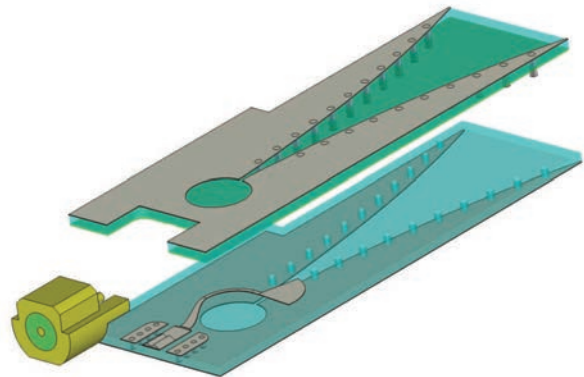


Fig. 5. Antenna element consisting of two substrates. microstrip feed placed in between substrates

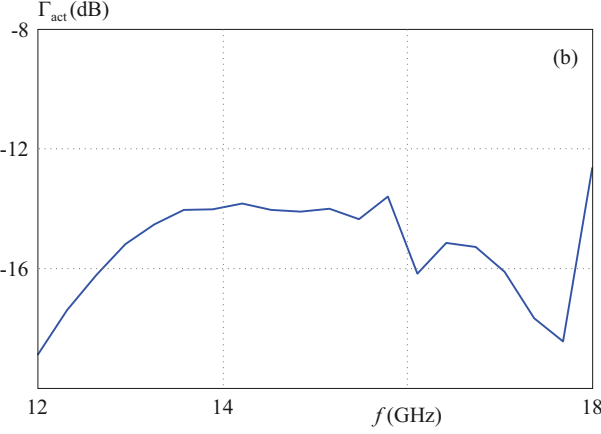
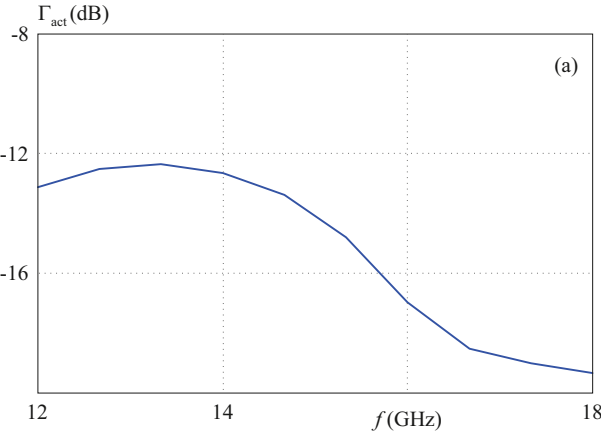


Fig. 6. Frequency response of reflection coefficient at the input of single-layer Vivaldi element (top) and double-layer one (bottom)

see Fig. 5. Due to the higher computational complexity of this model, the element was used in an antenna array with a reduced number of elements.

The Vivaldi element is of the dimensions 26 mm \times 8 mm. Since the design is a part of intellectual property, all the dimensions of the basic antenna element are not allowed to be published.

Simulated frequency responses of reflection coefficient at the input of a single-layer element and a double-layer

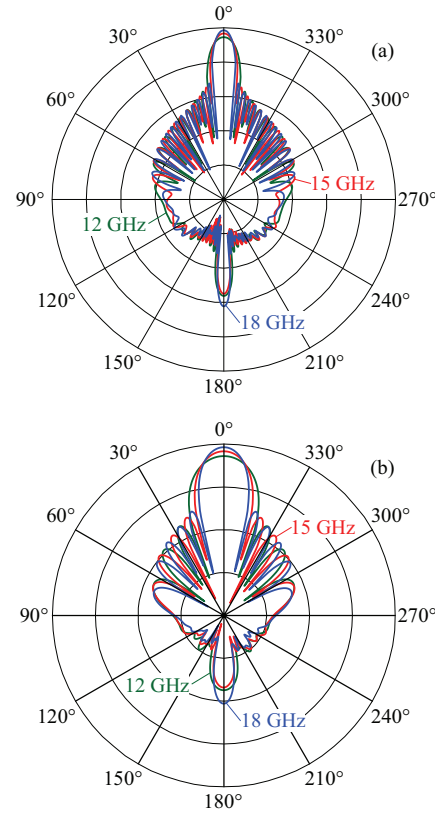


Fig. 7. Radiation pattern of 32×16 cells from single-layer perpendicular Vivaldi slots horizontal plane (top), vertical plane (bottom)

one are depicted in Fig. 6. Simulations were performed for scanning angles $\pm 20^\circ$ in the horizontal plane to verify the possibility of the beam control.

2.1 32×16 antenna array

An array consisting of 32×16 cells was created from single-layer perpendicular Vivaldi slots. This model should serve for a numerical analysis of the possibility to obtain the required gain and beam width.

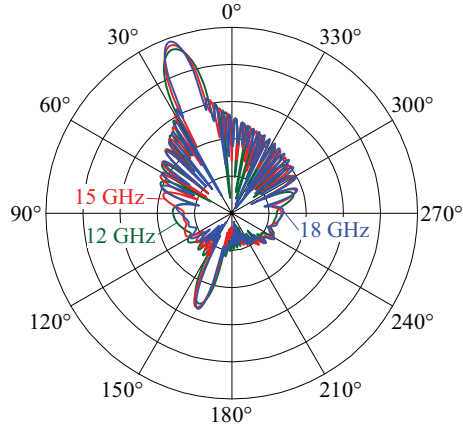


Fig. 8. Beam steering of 32×16 array by phase shifting

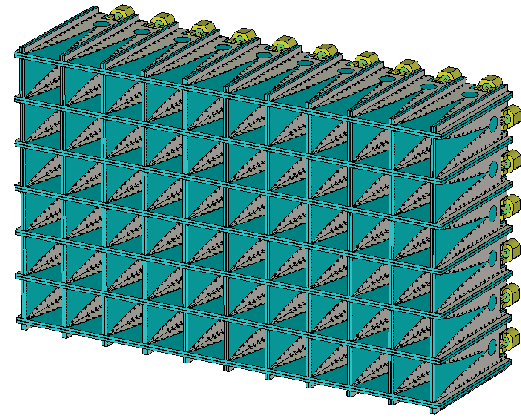


Fig. 9. The array of 8×4 active elements surrounded by row of passive elements

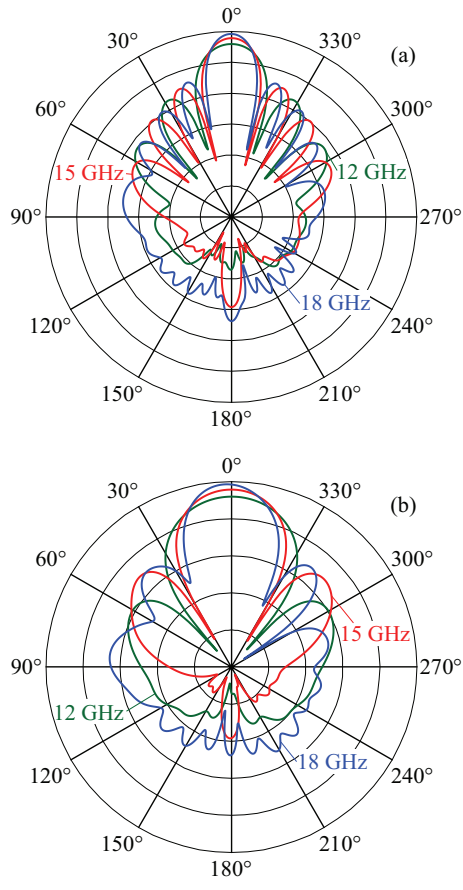


Fig. 10. Radiation pattern of 8×4 cells from double-layer perpendicular Vivaldi slots horizontal plane (top), vertical plane (bottom)

Due to the size of the array, the distribution of amplitudes on individual elements followed Taylor series to suppress side lobes. The substrate Rogers RT5880 with 0.254 mm thickness was used.

Figure 7 shows radiation patterns in the horizontal plane (top) and the vertical planes (bottom) for three significant frequencies. A large number of side lobes are visible. Their suppression is about 25 dB, the beam width 5.4° in the horizontal plane and the gain is 27 dB at the

central frequency 15 GHz. For better clarity of the shape of patterns, no gain values are given in figures.

The antenna array should provide the ability to control the main beam in the horizontal plane by phase shifting of neighbouring elements as demonstrated in Fig. 8. Here, the main beam is steered by 20° in the horizontal plane.

As shown in [3], the beam steering can cause the formation of a parasitic side lobe on the opposite side of the main-lobe half-space. This effect can be suppressed by the optimization of the slot length L . But in that case, we can observe only the parasitic back lobe as in Fig. 7. This back lobe can be further suppressed by an additional shielding.

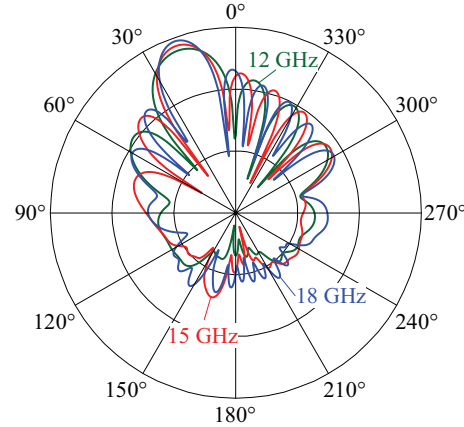


Fig. 11. Beam steering of 8×4 array by phase shifting

2.2 8×4 antenna array

To reduce the computational complexity, a smaller antenna array consisting of 8×4 cells was created from double-layer perpendicular Vivaldi slots. The array was simulated without a controlled amplitude distribution to suppress side lobes. Figure 9 shows that there is an additional row of antenna elements terminated by 50Ω loads around the whole antenna array. These passive elements help to minimize boundary effects and ensure a better suppression of side lobes. The substrate Rogers

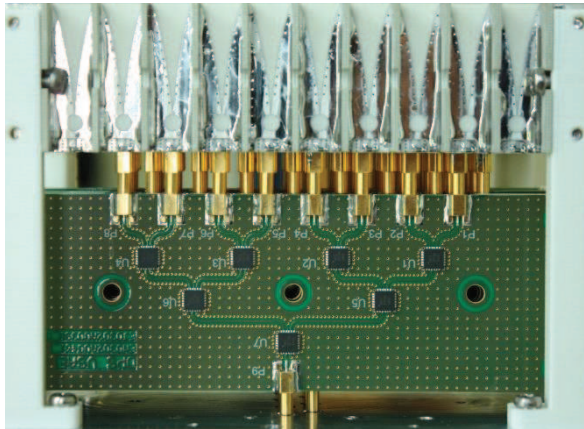


Fig. 12. Implemented feeding network with on-chip power dividers

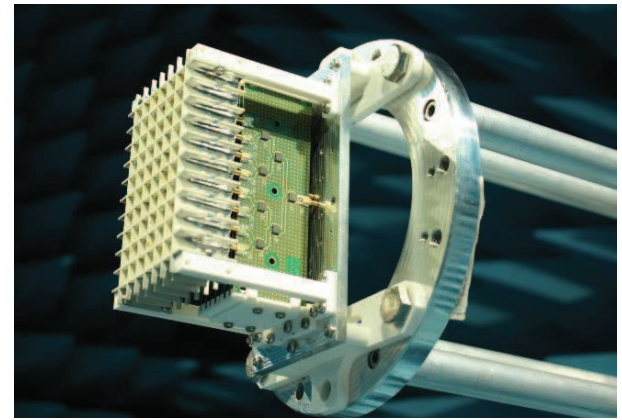


Fig. 13. Complete antenna array measured in anechoic chamber

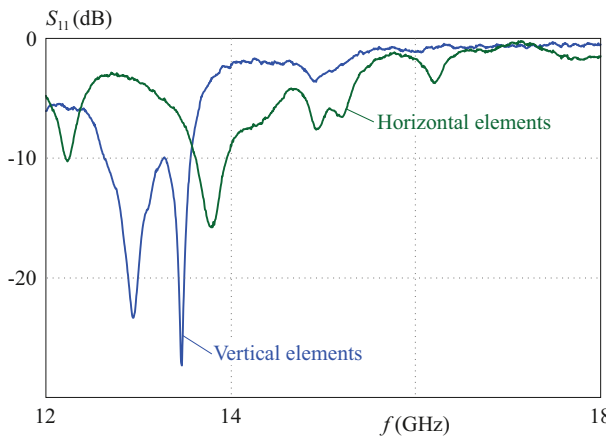


Fig. 14. Measured frequency response of reflection coefficient: vertical polarization (blue), horizontal polarization (red)

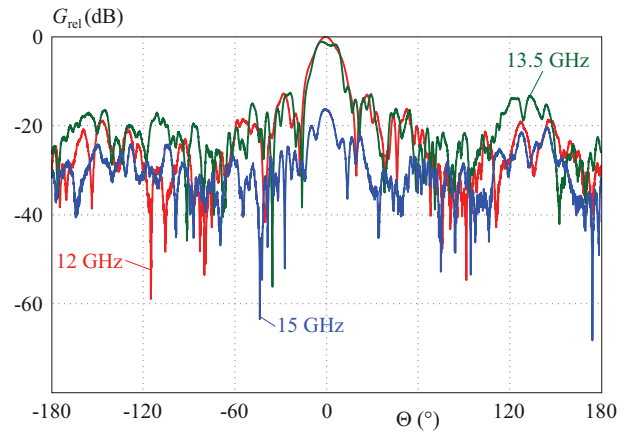


Fig. 15. Measured radiation pattern of vertical elements in horizontal plane

RO4730JXR with 0.526 mm thickness was considered. The model was subsequently used to manufacture the first prototype.

The radiation pattern of the 8×4 array, see Fig. 10, shows the expected decrease of the number of side lobes as well as their worse suppression. The 13 dB side lobe level agrees with theory - an antenna array of more than eight elements cannot achieve better side lobe level than 13.26 dB [4]. Due to the smaller number of elements in the array, the beam width in the horizontal plane is 13.3° and the gain at 15 GHz was decreased to 17.9 dB. Obviously worse parameters correspond to the smaller number of elements and a uniform distribution of amplitudes. Radiation pattern in Fig. 11 shows that the main beam steering does not cause the extra parasitic side lobe mirrored to the main beam. In order to implement the designed arrays, a proper feeding network has to be developed.

3 Power dividing network

The final array contains a high number of active antenna elements - 512 cells in case of the 32×16 array

(1024 active antenna elements for vertical and horizontal polarizations together). Hence, the design of the feeding network is quite demanding. We used a model of the multistage Wilkinson power divider and simulated it with good results. These power dividers can be cascaded for all antenna elements. But for the first prototype of the array was decided to be fed by a conventional feeding network based on chip power dividers EPK2+ by Mini Circuits [9].

4 Prototype

In order to manufacture the prototype, the array of 8×4 elements was used. The array was completed by the feeding system with two inputs for separate polarizations. The whole structure in the mounting bracket is shown in Fig. 13. To reduce the costs, no main beam steering was implemented in the first prototype.

4.1 Measurements

The antenna array was measured in an anechoic chamber in the whole frequency band for both the polariza-

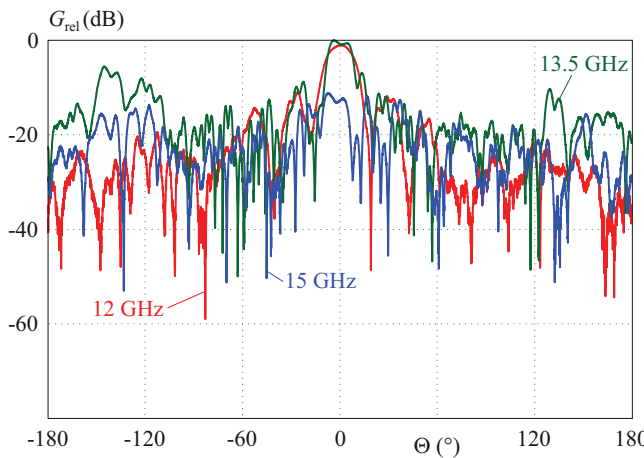


Fig. 16. Measured radiation pattern of horizontal elements in horizontal plane

tions. Impedance characteristics were measured on both the inputs of the antenna array for vertical and horizontal elements (see Fig. 14). Obviously, impedance matching of the antenna array is not acceptable. In laboratory, we revealed problems with soldering chip power dividers causing these bad values.

Considering the measured impedance matching, the gain was measured only at lower frequencies. As expected, the obtained gain deviated from simulations. At 12 GHz, the measured gain of vertical elements was 8.15 dBi compared to 16 dBi in simulation.

Nevertheless, the measurement was useful. Fig. 15 shows that we were able to obtain the main beam width of 14° in the horizontal plane (the essential one) for vertical elements. The side-lobe suppression at 12 GHz with the value of 12.8 dBi is also satisfactory (the simulated value was 13 dBi). The values of gain are related to the main lobe gain (8.15 dBi).

Similarly, Fig. 16 shows the gain in the horizontal plane for horizontal elements. The gain at 12 GHz was 4.8 dBi which is insufficient. The side-lobe suppression at 12 GHz was 10 dB and the main beam width was 17° showing a reasonable agreement with simulations. At 13.5 GHz, there is a noticeable high level of side lobes caused by impedance mismatch of central elements for this frequency.

5 Conclusion

In the paper, a concept of an antenna array based on Vivaldi antenna elements was presented. The design was optimized for requested gain, beam width, sidelobe level,

impedance matching, phase-shift steering and mechanical stability. To meet the requirements, a double-layer antenna element with microstrip feeding in between layers was proposed. The antenna can be manufactured by common etching of microwave substrates.

Parameters of the proposed array were verified by computer simulations and validated by a simple experiment. For measurements, an array of 8×4 active elements was surrounded by a row of passive elements. The array was completed by a feeding network based on chip power dividers. Due to the problems with soldering, measured results were significantly worse compared to measurements.

Even the prototype did not meet the given requirements, there is a good assumption to achieve the required parameters with proper modifications of the power dividing network. Network optimization could be as demanding as the design of the antenna array.

After solving problems, the antenna array can be completed by the system of distributed amplitudes for better side lobe suppression and by phase shifters to obtain beam steering in the horizontal plane.

Acknowledgments

The presented research was supported by the Internal Grant Agency of Brno University of Technology, the project no. FEKT-S-20-6526.

REFERENCES

- [1] P. J. Gibson, "The Vivaldi Aerial", *9th European Microwave Conference*, pp. 101–105, 1979.
- [2] C. A. Balanis, *Antenna theory: Analysis and design*, 3rd ed., Hoboken: Wiley-Interscience, 2005.
- [3] F. B. Gross, Ed. *Frontiers antennas*, New York, McGraw-Hill, 2011.
- [4] J. D. S. Langley, P. S. Hall, and P. Newham, "Balanced Antipodal Vivaldi Antenna for Wide Bandwidth Phased Arrays", *IEE Proceedings – Microwaves, Antennas and Propagation*, vol. 143, no. 2, 1996.
- [5] M. Huang, L. Zhang, W. Wang, and Qiao, "An Ultrawideband Tightly Coupled Antipodal Vivaldi Antenna Array for UHF-Ku Band Applications", pp. 1323–1324, 2017.
- [6] R. Hahnel and D. Plettmeier, "Dual-polarized Vivaldi Array for X- and Ku-Band", *Proceedings of the 2012 IEEE International Symposium on Antennas and Propagation*, pp. 1–2, 2012.
- [7] E. Hanbay and M. E. Aydemir, "High Gain Ultrawide Band Vivaldi Antenna Design for Mini/Micro Satellite Synthetic Aperture Radar Applications", *9th International Conference on Recent Advances Space Technologies (RAST)*, pp. 491–495, 2019.
- [8] R. C. Hansen, *Phased array antennas*, 2nd ed., Hoboken, N. J., Wiley, 2009.
- [9] Power Splitter/Combiner EP2K+ Mini-Circuits.

Received 20 April 2020